Rapid Kinetics of Tyrosyl Radical Formation and Heme Redox State Changes in Prostaglandin H Synthase-1 and -2

ARTICLE *in* JOURNAL OF BIOLOGICAL CHEMISTRY · AUGUST 1999

Impact Factor: 4.57 · DOI: 10.1016/S0090-6980(99)90355-6 · Source: PubMed

7 AUTHORS, INCLUDING:

Ah-Lim Tsai
University of Texas Health Science Center at…
142 PUBLICATIONS **4,604** CITATIONS
SEE PROFILE

Gang Wu
University of Texas Health Science Center at…
30 PUBLICATIONS **462** CITATIONS
SEE PROFILE

THE JOURNAL OF BIOLOGICAL CHEMISTRY
Vol. 274, No. 31, Issue of July 30, pp. 21695–21700, 1999

Printed in U.S.A.

Rapid Kinetics of Tyrosyl Radical Formation and Heme Redox State Changes in Prostaglandin H Synthase-1 and -2*

(Received for publication, April 2, 1999, and in revised form, May 20, 1999)

Ah-lim Tsai‡§, Gang Wu‡, Graham Palmer¶, Bijan Bambai‡, James A. Koehn‖, Paul J. Marshall‖, and Richard J. Kulmacz‡

From the ‡Division of Hematology, Department of Internal Medicine, University of Texas Health Science Center, Houston, Texas 77030, the ¶Department of Biochemistry and Cell Biology, Rice University, Houston, Texas 77005, and the ‖Arthritis Research Department, Novartis Pharmaceuticals, Summit, New Jersey 07901

Hydroperoxide-induced tyrosyl radicals are putative intermediates in cyclooxygenase catalysis by prostaglandin H synthase (PGHS)-1 and -2. Rapid-freeze EPR and stopped-flow were used to characterize tyrosyl radical kinetics in PGHS-1 and -2 reacted with ethyl hydrogen peroxide. In PGHS-1, a wide doublet tyrosyl radical (34–35 G) was formed by 4 ms, followed by transition to a wide singlet (33–34 G); changes in total radical intensity paralleled those of Intermediate II absorbance during both formation and decay phases. In PGHS-2, some wide doublet (30 G) was present at early time points, but transition to wide singlet (29 G) was complete by 50 ms. In contrast to PGHS-1, only the formation kinetics of the PGHS-2 tyrosyl radical matched the Intermediate II absorbance kinetics. Indomethacin-treated PGHS-1 and nimesulide-treated PGHS-2 rapidly formed narrow singlet EPR (25–26 G in PGHS-1; 21 G in PGHS-2), and the same line shapes persisted throughout the reactions. Radical intensity paralleled Intermediate II absorbance throughout the indomethacin-treated PGHS-1 reaction. For nimesulide-treated PGHS-2, radical formed in concert with Intermediate II, but later persisted while Intermediate II relaxed. These results substantiate the kinetic competence of a tyrosyl radical as the catalytic intermediate for both PGHS isoforms and also indicate that the heme redox state becomes uncoupled from the tyrosyl radical in PGHS-2.

Prostaglandin H synthase (PGHS)[1] catalyzes the first committed step in the biosynthesis of prostanoids. There are two isoforms of PGHS, with the constitutive form (PGHS-1) ascribed housekeeping functions and the inducible form (PGHS-2) associated with cytokine-mediated pathophysiological events (1, 2). Although the isoforms share only 60% sequence identity, their overall three-dimensional structures are very similar, especially in the catalytic sites (3–5). Both isoforms exhibit two enzymatic activities: a cyclooxygenase activity, which converts arachidonic acid to prostaglandin G_2, and a peroxidase activity, which transforms prostaglandin G_2 to prostaglandin H_2. Several oxidized reaction intermediates have been identified (6–9). As indicated in Scheme 1, PGHS first interacts with a peroxide substrate, such as prostaglandin G_2, to generate Intermediate I, equivalent to Compound I of horseradish peroxidase. Intermediate I then converts to Intermediate II, equivalent to complex ES of cytochrome *c* peroxidase, through an intramolecular electron transfer from a tyrosine residue to the oxidized porphyrin. The transient tyrosyl radical in Intermediate II in each PGHS isoform is capable of oxidizing arachidonic acid to generate an arachidonic acid radical and initiate cyclooxygenase catalysis (10, 11). Crystallographic data revealed that the presumed site of the tyrosyl radical, Tyr-385 in PGHS-1 (Tyr-371 in PGHS-2), is located between the heme and arachidonate binding sites, well positioned to couple the two enzyme activities (3–5), as proposed in the original branched-chain mechanism (7, 8) (Scheme 1).

Although the chemical competence of the tyrosyl radical for cyclooxygenase catalysis has been convincingly demonstrated by single-turnover experiments (10, 11), the kinetic competence of the tyrosyl radical had been examined only with manual mixing techniques (13). Thus, the relationship between tyrosyl radical kinetics and those of the rapid changes in the heme redox state during PGHS peroxidase reactions remained unresolved. The redox linkage between the heme center and the tyrosyl radical needs to be defined to determine the coupling efficiency between the two enzyme activities.

Several types of tyrosyl radical EPR spectra have been observed in the PGHS isozymes (Refs. 7, 12–16 and Table I). A 33–35-G wide doublet (WD1) and wide singlet (WS1) are observed when PGHS-1 is manually mixed with various hydroperoxides (12). On the other hand, only a 29-G wide singlet (WS2) is found in PGHS-2 for similar manually mixed peroxidase reactions (16, 24). It was of interest to know whether the lack of observable WD in PGHS-2 was the result of a fundamentally different tyrosyl radical structure in this isoform or of a more rapid transition to a wide singlet. The peroxidase reaction in PGHS-1 treated with cyclooxygenase inhibitors such as aspirin, indomethacin, and flurbiprofen or with the mutation of Tyr-385 to phenylalanine resulted in the formation of a 25–26-G narrow singlet (NS1a) (12, 17, 18). A similar 21-G narrow singlet (NS2a) was observed for PGHS-2 treated with the cyclooxygenase inhibitor nimesulide or with the mutation of Tyr-371 (11, 16). These observations of a perturbed tyrosyl radical EPR in PGHS-1 and -2 with impaired cyclooxygenase activity were from manually mixed samples. It remained important to determine whether other radicals were generated earlier in the rapid reactions with peroxide.

We have used rapid-freeze EPR to measure the tyrosyl radical kinetics during reaction of PGHS-1 and -2 with EtOOH,

* This work was supported by United States Public Health Service Grants GM44911 (to A.-L. T.), GM52170 (to R. J. K.), and GM21337 (to G. P.) and by Welch Foundation Grant C636 (to G. P.). The costs of publication of this article were defrayed in part by the payment of page charges. This article must therefore be hereby marked "*advertisement*" in accordance with 18 U.S.C. Section 1734 solely to indicate this fact.

§ To whom correspondence should be addressed: Div. of Hematology, University of Texas Health Science Center, P. O. Box 20708, Houston TX 77225. E-mail: atsai@heart.med.uth.tmc.edu.

[1] The abbreviations used are: PGHS-1, ovine prostaglandin H synthase-1; EtOOH, ethyl hydrogen peroxide; WD, wide doublet tyrosyl radical; WS, wide singlet tyrosyl radical; NS, narrow singlet tyrosyl radical; EPR, electron paramagnetic resonance; ENDOR, electron nuclear double resonance.

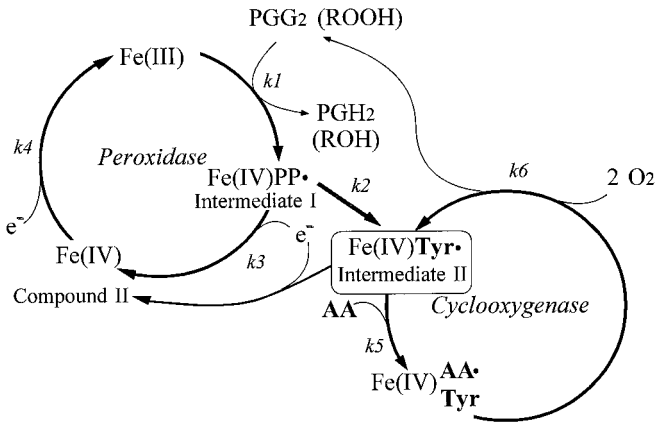

SCHEME 1. **Branched-chain radical mechanism of PGHS.** *AA*, arachidonic acid; *PGG_2*, prostaglandin G_2; *PGH_2*, prostaglandin H_2; *ROOH* and *ROH*, hydroperoxide and corrresponding alcohol.

TABLE I
Tyrosyl radical EPR species in PGHS-1 and -2

Nomenclature	Origin	EPR features
WD1	Wide doublet in PGHS-1	34–35 G, 19 G splitting
WD2	Wide doublet in PGHS-2	30 G
WS1	Wide singlet in PGHS-1	33–35 G
WS2	Wide singlet in PGHS-2	29 G
NS1a	Narrow singlet in PGHS-1 treated with cyclooxygenase inhibitor	25–26 G, hyperfine structure
NS1b	Narrow singlet in self-inactivated PGHS-1	25–28 G, no hyperfine features
NS2a	Narrow singlet in PGHS-2 treated with cyclooxygenase inhibitor	21 G

both with and without pretreatment of the enzymes with cyclooxygenase inhibitors. Parallel stopped-flow measurements were done to determine the kinetics of Intermediate I and II formation. The results indicate that very rapid formation of WD species coincides with formation of Intermediate II in both PGHS-1 and -2, consistent with the proposed mechanism (Ref. 7 and Scheme 1), and the formation of the narrow singlet EPR coincides with Intermediate II formation in the isozymes treated with cyclooxygenase inhibitors.

EXPERIMENTAL PROCEDURES

Phenol, indomethacin, flurbiprofen, nimesulide, and hemin were purchased from Sigma. EtOOH was purchased as a 5% aqueous solution from Polysciences Inc. (Warrington, PA) or from Accurate Chemical and Scientific Corp. (Westbury, NY) as a 10% solution. EtOOH concentrations were determined from the absorbance at 230 nm using an extinction coefficient of 43 M^{-1} cm^{-1}. Tween 20 was purchased from Pierce.

PGHS-1 was prepared as the apoenzyme from ram seminal vesicles, with 5 mM glutathione included in the isoelectric focusing step (9, 20). Recombinant human PGHS-2 was expressed in a baculovirus system using Sf9 or High Five (Invitrogen) insect cells and purified as described previously (21). PGHS holoenzymes were formed by adding excess heme to the apoenzyme followed by treatment with DE52 cellulose (Whatman) and gel filtration on a Bio-Rad 10-DG column (for PGHS-1) or gel filtration alone (for PGHS-2). A minimal amount of phenol (50 μM) was added to PGHS-2 during reconstitution to avoid loss of activity. The concentration of PGHS holoenzyme was based on the absorbance at 411 nm for PGHS-1 and at 408 nm for PGHS-2 (165 mM^{-1} cm^{-1}).

The cyclooxygenase specific activity, assayed polarographically at 30 °C (20), was 80–120 μmol of O_2/min/mg for PGHS-1 and 10–30 μmol of O_2/min/mg for PGHS-2.

Optical stopped-flow kinetic measurements were conducted using a Bio-SEQUENTIAL DX-18MV stopped-flow instrument (Applied Photophysics, Leatherhead, UK). Wavelength pairs of 428 and 524 nm (isosbestic points between resting PGHS-1 and Intermediate I (8, 9)) were used to monitor changes in Intermediate II in PGHS-1. In the case of PGHS-2, the large value of k_2 (conversion of Intermediate I to Intermediate II) resulted in a minimal accumulation of Intermediate I, and so there was hardly any observable accumulation of Intermediate I (26). We thus chose to monitor Intermediate II kinetics in PGHS-2 at 406 and 428 nm.

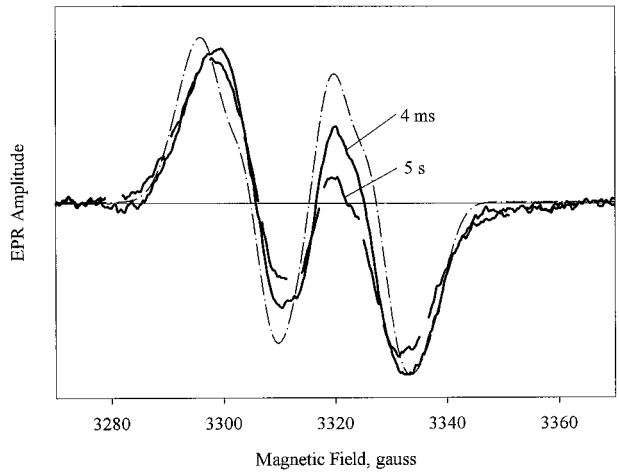

FIG. 1. **WD tyrosyl radical EPR spectra from reaction of PGHS-1 with EtOOH.** PGHS-1 (15 μM) was reacted at room temperature with 30 μM EtOOH in 0.1 M potassium phosphate, pH 7.2, with 10% glycerol and 0.1% Tween 20. EPR spectra were acquired as described under "Experimental Procedures" for samples freeze-trapped at 4 ms (*thick solid line*) and 5 s (*thick dashed line*). The *thin dashed-dotted line* is a computer-simulated spectrum using the WD1 parameters obtained from ENDOR studies[2]: g_x = 2.0064, g_y = 2.0044, g_z = 2.0023; A_{xx} = 21.6 G, A_{yy} = 22.8 G, and A_{zz} = 22.8 G for the beta carbon hydrogen; A_{xx} = 9.52, A_{yy} = 2.74, and A_{zz} = 7.22 G for the 3-, and 5-phenyl hydrogens, with a line width of 3 G.

Rapid-freeze experiments were conducted using a System 1000 chemical/freeze quench apparatus with a Model 1019 syringe ram, a Model 715 ram controller, and an 0.008-in nozzle (Update Instrument, Inc. Madison, WI). A low temperature isopentane bath was used for pre-chilling the packing assembly containing isopentane and later for cooling during sample packing via a pressure filtration process developed recently in our laboratory (19). The bath temperature was kept at 125–130 K, bringing the temperature of isopentane inside the funnel to 130–135 K. The temperatures were monitored with a silicon diode temperature sensor (Lakeshore model 200 monitor with a DT-471-PA1 probe). Unless otherwise mentioned, the ram velocity was 2 cm/s in all rapid-mixing experiments. Single-push mixing was used for reactions of less than 160 ms; longer reactions used a push-push mixing syringe program. The dead time of the apparatus, measured with myoglobin-azide reactions, is 4–5 ms (19). EPR spectra of samples collected from rapid-freeze experiments were recorded with a Varian E-6 spectrometer. The EPR conditions were as follows: modulation amplitude, 3.2 G; time constant, 1 s; power 1 mW; and temperature, 96 K. Radical concentrations were determined by double integration of the EPR signal using a copper standard (12) and a packing correction factor of 0.45 determined earlier for this system (19).

RESULTS

Kinetics of PGHS-1 Tyrosyl Radicals—To observe the earliest possible events in tyrosyl radical formation, we reacted PGHS-1 with two equivalents of EtOOH at 0 °C and freeze-trapped the sample at various reaction times. The sample trapped at 4 ms showed a typical wide-doublet tyrosyl radical (WD1) with a peak-to-trough width of 34 G and a well resolved 19-G center splitting (Fig. 1). A sample trapped after 5 s of reaction still showed a doublet spectrum but with some decay of the center splitting. Comparison of the freeze-trapped samples with the wide-doublet EPR predicted from the parameters obtained in electron nuclear double resonance (ENDOR) meas-

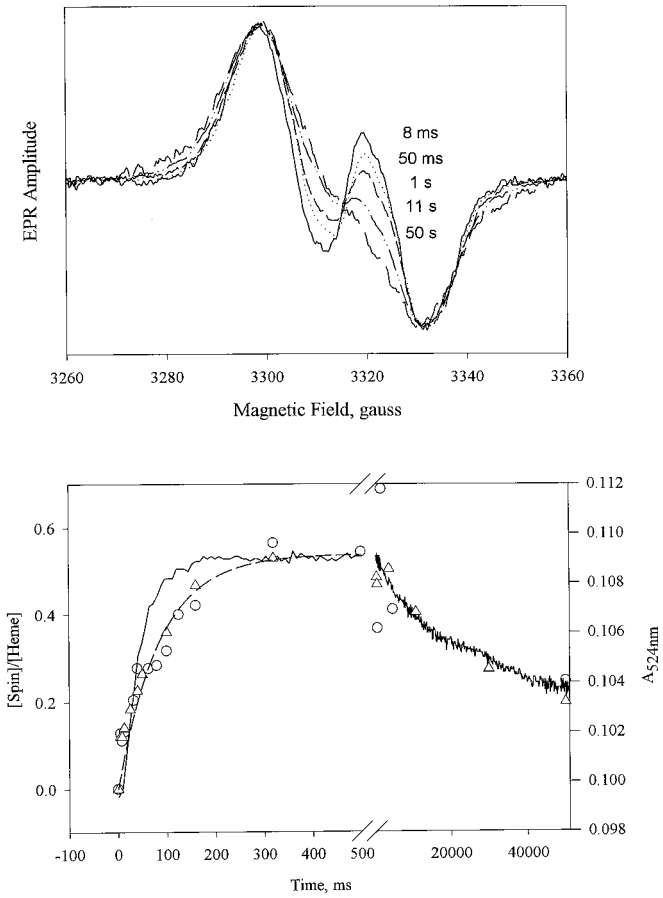

FIG. 2. **Radical and ferryl heme kinetics during reaction of PGHS-1 with EtOOH.** *Top panel*, PGHS-1 (8.5 μM) was reacted with 42 μM EtOOH for the indicated time periods before freeze-trapping and EPR analysis. The EPR spectra were normalized to the same amplitude and overlaid to facilitate line shape comparisons. *Bottom panel*, radical intensities were determined by double integration of the EPR spectra and plotted as a function of reaction time. *Circles* and *triangles* denote data from two separate experiments. The kinetics of ferryl heme (*solid line*) were determined by stopped-flow measurements at 524 nm in parallel reactions of PGHS-1 with EtOOH under the same conditions used for EPR measurements. The *smooth dashed line* is the single-exponential fitting to the data of tyrosyl radical intensity.

urements[2] indicates that the center splitting in the WD1 EPR had already declined by ~30% at 4 ms (Fig. 1).

Increasing the ratio of EtOOH/PGHS-1 to 5 and raising the temperature permitted observation of a more complete transition from WD1 to a wide singlet tyrosyl radical (WS1) (Fig. 2, *top*). This transition was essentially complete within 50 s. The initial formation of tyrosyl radical was rapid (k = 16 s^{-1}) and reached a plateau at ~0.6 spin/heme within 300 ms (Fig. 2, *bottom*). A slow decay in radical intensity (k = 0.047 s^{-1}) began after about 500 ms (Fig. 2, *bottom*). The kinetics of Intermediate II, monitored at A_{524}, closely tracked those of the tyrosyl radical. The rate of Intermediate II formation was 24 s^{-1} (Fig. 2, *bottom*). These results indicate a tight redox linkage between the heme center and the tyrosyl radical in PGHS-1. The slight difference in formation rates between tyrosyl radical and Intermediate II probably originates in the different methods used for their measurement, but it might also imply an additional step occurring between formation of Intermediate II and tyrosyl radical. Stopped-flow observations at 428 nm paralleled those at 524 nm in the early phase but showed a more rapid

[2] W. Shi, C. W. Hoganson, M. Espe, C. J. Bender, G. T. Babcock, G. Palmer, R. J. Kulmacz, and A.-L. Tsai, submitted for publication.

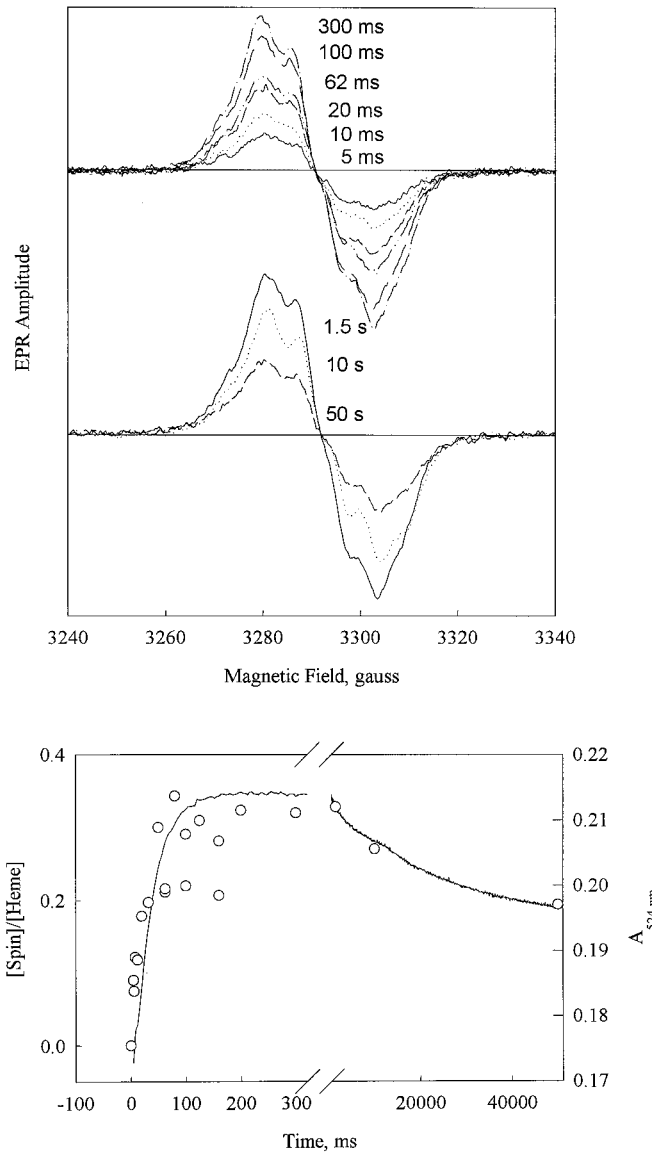

FIG. 3. **Radical and ferryl heme kinetics during reaction of indomethacin-treated PGHS-1 with EtOOH.** *Top panel*, indomethacin-treated PGHS-1 (15.8 μM) was reacted with 5 eq of EtOOH at 24 °C for the indicated times and freeze-trapped for acquisition of the EPR spectra. The same vertical scale was used for the spectra from the formation (*upper*) and decay (*lower*) phases with no normalization. *Bottom panel*, tyrosyl radical intensities (*circles*) were determined by double integration of the EPR signals and presented with the ferryl heme kinetics monitored at A_{524} in parallel stopped-flow experiments (*solid line*).

decay (data not shown), indicating that additional events, such as self-inactivation, were also detected at this wavelength (25).

Effects of Cyclooxygenase Inhibitors on PGHS-1 Tyrosyl Radical Kinetics—The EPR spectra of samples trapped at various times during reaction of indomethacin-treated PGHS-1 and EtOOH (5 eq) all showed a 25–26-G narrow singlet (NS1a) with discrete hyperfine features (Fig. 3, *top*) just as was found earlier in manual mixing experiments (12, 17). There was no indication of initial formation of either WD1 or WS1 signals. Formation of the NS1a radical was rapid (k = 47 s^{-1}) and reached a plateau at ~0.35 spin/heme within 200 ms, followed by a slow relaxation (Fig. 3, *bottom*). As in the case of PGHS-1 itself, the kinetics of Intermediate II (29 s^{-1} for the initial phase) paralleled those of the NS1a radical, indicating that binding of indomethacin did not disrupt the redox linkage between the heme and the tyrosyl radical. Separate experi-

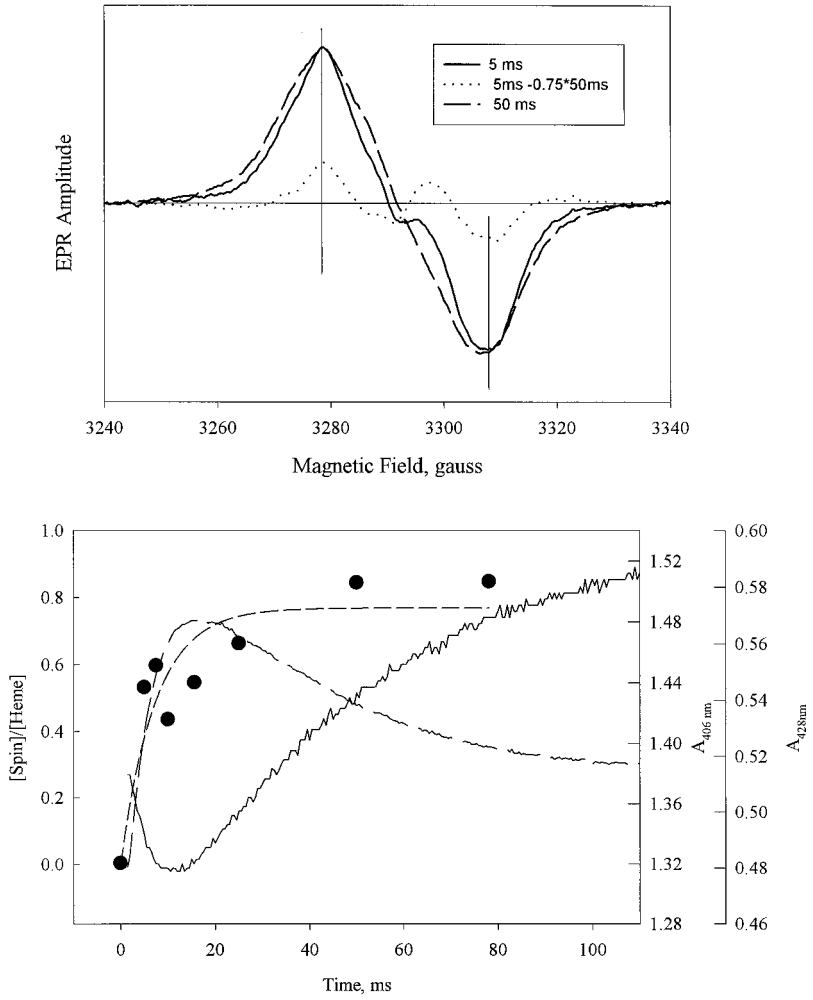

FIG. 4. **Radical and ferryl heme kinetics during reaction of PGHS-2 with EtOOH.** PGHS-2 (11.2 μM) in 0.1 M potassium phosphate, pH 7.2, containing 0.1% Tween 20 and 10% glycerol was reacted with 56 μM EtOOH at 24 °C. *Top panel*, EPR spectra were acquired for samples freeze-trapped at 5 (*solid line*) and 50 ms (*dashed line*) and normalized to the same amplitude. The *dotted line* is the difference spectrum obtained by subtracting 75% of the 50-ms spectrum from the 5-ms spectrum. *Bottom panel*, the kinetics of the tyrosyl radical (*solid circles* and *short-dashed line* for a single-exponential fit) were obtained by double integration of the EPR spectra. The heme kinetics were monitored in parallel stopped-flow experiments monitored at 406 (*continuous line*) and 428 nm (*long dashes*).

ments using flurbiprofen instead of indomethacin gave very similar results for both the tyrosyl radical and Intermediate II kinetics (data not shown).

Kinetics of PGHS-2 Tyrosyl Radicals—Substantial formation of tyrosyl radicals was evident at the earliest stage (5 ms) of reaction of PGHS-2 with 5 eq of EtOOH (Fig. 4, *top*). The EPR spectrum of the initial sample exhibited a complex, 29–30-G wide signal with a clearly discernible splitting, whereas the spectrum of the sample at 50 ms was essentially a simple singlet (WS2), indicating a very rapid transition from doublet to singlet in PGHS-2. Subtraction of 75% of the signal intensity of the 50-ms sample from the 5-ms sample EPR yielded a doublet with a peak-to-trough width of 30 G (Fig. 4, *top*), indicating the presence of a substantial wide doublet tyrosyl radical in the very early stages of the PGHS-2 peroxidase reaction.

The formation of tyrosyl radical in PGHS-2 was rapid (~140 s^{-1}). The radical intensity reached a plateau near 0.8 spin/heme by ~50 ms and remained at this level for at least 100 ms (Fig. 4). Formation of Intermediate II, monitored by absorbance changes at 406 or 428 nm, was also rapid (~240 s^{-1}). In contrast to the persistent radical intensity, Intermediate II quickly relaxed back to the ferric heme (17–19 s^{-1}). This difference in behavior between the heme center redox state and the tyrosyl radical was observed for PGHS-2 but not PGHS-1 (compare Figs. 2 and Fig. 4).

The PGHS-2 preparation used above included 50 μM phenol as a protectant, and therefore the possible effect of phenol on the PGHS-1 tyrosyl radical and Intermediate II kinetics was examined. In the presence of phenol the rates of tyrosyl radical and Intermediate II formation (18 and 26 s^{-1}, respectively) were similar to those for phenol-free PGHS-1 reactions (Figs. 2 and 5). The maximal tyrosyl radical intensity in the presence of phenol was ~0.4 spin/heme, somewhat less than in the experiment done without phenol (Figs. 2 and 5). The presence of phenol resulted in a slower transition from WD1 to WS1, evident from the center inflection present in the EPR even after 330 ms (Fig. 5, *top*). This finding contrasts with the almost complete collapse of the center splitting pattern in the phenol-free PGHS-1 reactions (Fig. 2, *top*). A comparison of the PGHS-1 and -2 results in the presence of phenol indicated that the transition from wide doublet to wide singlet and the relaxation of Intermediate II were both slower in PGHS-1 (Figs. 4 and 5).

Tyrosyl Radical Kinetics in Nimesulide-treated PGHS-2—Reaction of nimesulide-treated PGHS-2 with 5 eq of EtOOH resulted in rapid formation of both the tyrosyl radical (176 s^{-1}) and Intermediate II (~ 350 s^{-1} from A_{428} observations) (Fig. 6). Intermediate II later decayed at a rate of 33 s^{-1} even though the tyrosyl radical intensity remained relatively constant (Fig. 6, *bottom*). The divergent decay kinetics of oxidized heme and tyrosyl radical were thus seen with both inhibitor-treated and native PGHS-2 (Figs. 4 and 6). The maximal intensity of the tyrosyl radical achieved in nimesulide-treated PGHS-2, ~0.4 spin/heme, was substantially lower than that found for PGHS-2 itself. EPR of samples collected throughout the reaction showed only the 21-G narrow singlet (NS2a), with no significant change in line shape (Fig. 6). There was no sign of

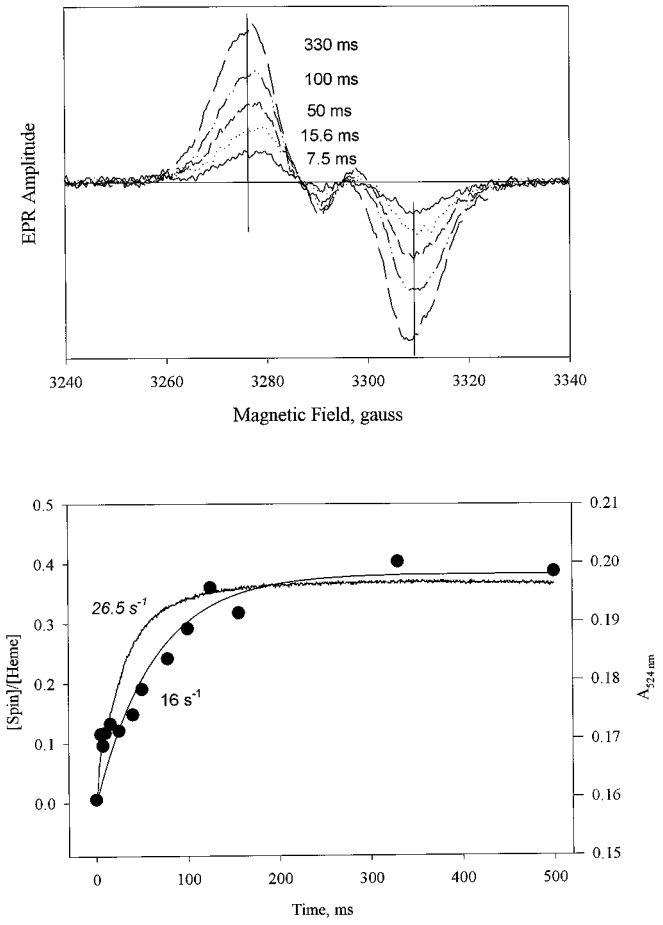

FIG. 5. **Tyrosyl radical and ferryl heme kinetics during reaction of PGHS-1 with EtOOH in the presence of phenol.** PGHS-1 (14.8 μM) in buffer supplemented with 50 μM phenol was reacted with 5 eq of EtOOH at 24 °C. *Top panel*, EPR spectra were acquired for samples freeze-trapped at the indicated reaction times. *Bottom panel*, tyrosyl radical intensities determined by double integration of the EPR spectra (*solid circles*) and presented with ferryl heme kinetics (*solid line*) monitored at 524 nm in parallel stopped-flow experiments. The *smooth solid line* denotes the single-exponential fit for the tyrosyl radical kinetic data.

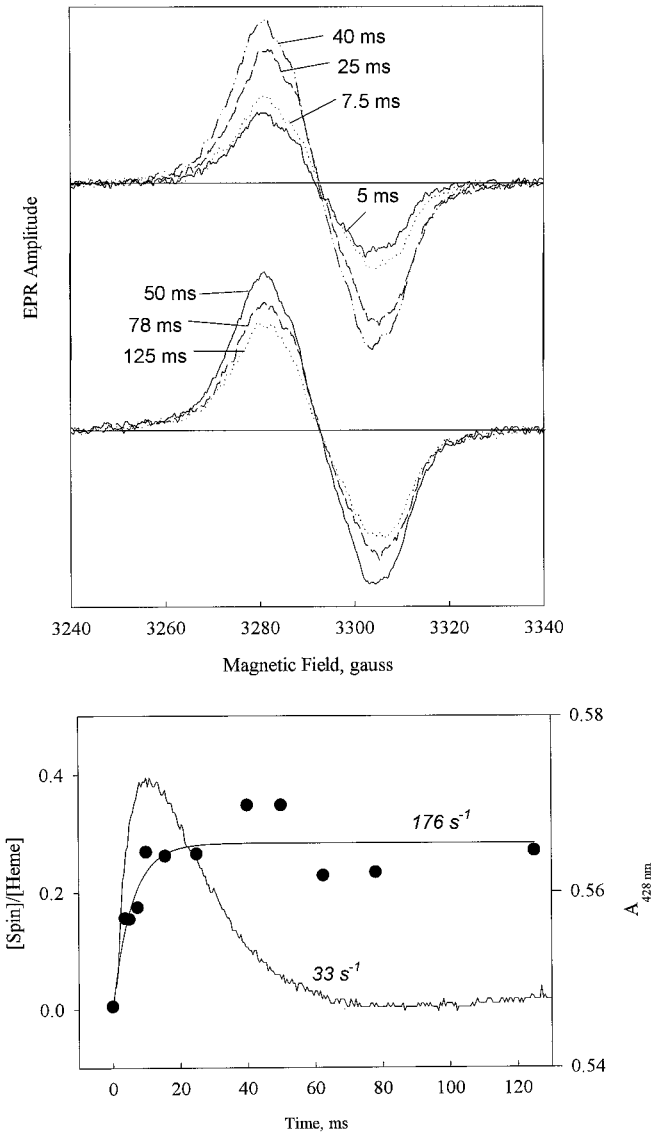

FIG. 6. **Tyrosyl radical and ferryl heme kinetics during reaction of nimesulide-treated PGHS-2 with EtOOH.** Nimesulide-treated PGHS-2 (8.4 μM) was reacted with 5 eq of EtOOH in the same buffer and under the same conditions as described in Fig. 4. *Top panel*, EPR spectra were acquired for freeze-trapped samples at the indicated reaction times. *Bottom panel*, tyrosyl radical intensities (*solid symbols*) were determined by double integration of the EPR spectra and are presented along with the kinetics of ferryl heme monitored in stopped-flow measurements at 428 nm in parallel reactions. The *smooth line* represents single-exponential fit to the tyrosyl radical intensity.

earlier formation of either a wide doublet or wide singlet, a situation similar to that with indomethacin-treated PGHS-1 (Figs. 3 and 6).

DISCUSSION

The rapid formation of WD and WS tyrosyl radicals observed in both PGHS-1 and -2 parallels the formation of the oxyferryl heme species (Intermediate II). This finding is just as predicted by the branched-chain radical mechanism originally proposed by Ruf and colleagues (7, 8). The kinetic competence of the tyrosyl radical for the proposed coupling of the peroxidase and cyclooxygenase activities in both of the PGHS isoforms is thus firmly established.

We previously examined the time-dependent changes of tyrosyl radical concentration and EPR line shape on a time scale of seconds using manual mixing at lower temperatures (-10 to 0 °C) (12, 13, 17). The slower kinetics observed in these earlier experiments probably reflects a previously unsuspected inefficiency in mixing the enzyme and peroxide in the narrow EPR tube by agitation with a nichrome wire loop. Earlier results from single-turnover experiments firmly established the chemical competence of the tyrosyl radical to oxidize arachidonic acid to a fatty acid radical (10, 11, 22, 23). It is clear from the present kinetic results that tyrosyl radicals in both of the PGHS isoforms are formed very rapidly, in concert with heme redox changes, just as expected from the proposed mechanism (Scheme 1). This result provides strong support for the mechanism and indicates that it accurately describes the events leading from the reaction with peroxide to the initiation of cyclooxygenase catalysis in both PGHS-1 and -2.

The present results also make it clear that a wide doublet tyrosyl radical (WD2) species is formed early in the reaction of peroxide with PGHS-2 just as with PGHS-1. The initial wide doublet undergoes a transition to a wide singlet in both isozymes, with a much faster rate for the transition in PGHS-2. Our ENDOR studies[2] support earlier reports (14, 15) that the WS1 of PGHS-1 is not a distinct species but is rather a mixture of the WD1 and a narrow-singlet (NS1b) associated with self-inactivated enzyme (13). This singlet is roughly similar to that seen with PGHS inhibited by anti-cyclooxygenase agents

(NS1a) but lacks the latter's detailed hyperfine features (13). Conditions that decrease PGHS-1 self-inactivation, such as decreasing the amount of EtOOH (Fig. 1) or including a reducing co-substrate (Fig. 5), significantly slowed the transition from WD to WS, consistent with the assignment of the NS1b signal to a tyrosyl radical in self-inactivated PGHS-1.

The structural interpretation for the WS observed in PGHS-2 (WS2) is ambiguous despite the general EPR similarities with the WS1 in PGHS-1. Definitive ENDOR data are not available for any of the PGHS-2 radical species. The narrower EPR line width of WS2 than of WS1 allows simulation of WS2 by simply increasing the dihedral angle between the p_z orbital of C1 and the C–H bond at the β carbon, corresponding to a change in coupling constant from 21 to 14 G for the β proton (16). This interpretation is consistent with WS2 arising from a distinct structural entity. However, it remains possible that WS2 is a mixture of a wide doublet and a narrow singlet, similar to WS1 in PGHS-1. ENDOR analysis of WS2 will be needed to decide between these two alternative structural interpretations and to understand the basis for the WD → WS transition observed in PGHS-2 (Fig. 4).

The present rapid-freeze EPR measurements did not detect formation of either WD or WS signals, even in the earliest stages of the peroxidase reaction, in either indomethacin-PGHS-1 or nimesulide-PGHS-2 (Figs. 3 and 6). This clear difference with the native isoforms strongly suggests that inhibitor treatment changes the pathway of intramolecular electron transfer in Compound I, resulting in oxidation of a surrogate tyrosine (exhibiting NS1a or NS2a EPR) rather than Tyr-385 (Tyr-371 in PGHS-2) during electron transfer to the heme porphyrin radical, as we previously proposed (18). The identity of this surrogate tyrosine residue is not known for either of the PGHS isoforms, although the similarity in power saturation between the NS1a and WD1 signals (12) and between the NS2a and WS2 signals (16) indicates similar environments for radicals on the surrogate tyrosine and on Tyr-385/Tyr-371.

The present kinetic data have revealed unexpected differences between the two isozymes in the redox association between the heme center and the tyrosyl radical (Figs. 2 and 4). Although formation of Intermediate II heme paralleled formation of tyrosyl radicals in both isozymes, the rate for PGHS-2 was faster than for PGHS-1. The faster rate of Intermediate II/tyrosyl radical formation for PGHS-2 fits with our recent comparative kinetic studies of these two isozymes, which showed PGHS-2 to have a much faster conversion from Intermediate I to II (26). Surprisingly, the redox relaxation of the tyrosyl radical and the heme center parallel one another in PGHS-1 but diverge markedly in PGHS-2 (Figs. 2 and 4). A similar difference was observed with the NS radicals in PGHS-1 and -2 treated with inhibitors (Figs. 3 and 6), with the redox relaxation of the tyrosyl radical and the heme center paralleling one another in PGHS-1 but diverging markedly in PGHS-2 (Fig. 2 and 4). This uncoupling of the tyrosyl radical redox state from the heme redox state in PGHS-2 may be physiologically significant because it tends to prolong the lifetime of the catalytically active tyrosyl radical and thus better sustain propagation of cyclooxygenase activity. This difference in redox coupling between oxyferryl heme and the tyrosyl radical in the two isoforms may contribute to the greater efficiency of hydroperoxide activation in PGHS-2 than in PGHS-1 (21).

Acknowledgments—We thank Dr. Guqiang Lu and Wei Chen for assistance in preparing the PGHS-2 enzyme.

REFERENCES

1. Smith, W. L., and DeWitt, D. L. (1996) *Adv. Immunol.* **62,** 167–215
2. Herschman, H. R. (1996) *Biochim. Biophys. Acta* **1299,** 125–140
3. Picot, D., Loll, P. J., and Garavito, R. M. (1994) *Nature* **367,** 243–249
4. Luong, C., Miller, A., Barnett, J., Chow, J., Ramesha, C., and Browner, M. F. (1996) *Nat. Struct. Biol.* **3,** 927–933
5. Kurumbail, R. G., Stevens, A. M., Gierse, J. K., McDonald, J. J., Stegeman, R. A., Pak, J. Y., Gildehaus, D., Miyashiro, J. M., Penning, T. D., Seibert, K., Isakson, P. C., and Stallings, W. C. (1996) *Nature* **384,** 644–648
6. Lambeir, A. M., Markey, C. M., Dunford, H. B., and Marnett, L. J. (1985) *J. Biol. Chem.* **260,** 14894–14896
7. Karthein, R., Dietz, R., Nastainczyk, W., and Ruf, H. H. (1988) *Eur. J. Biochem.* **171,** 313–320
8. Dietz, R., Nastainczyk, W., and Ruf, H. H. (1988) *Eur. J. Biochem.* **171,** 321–328
9. Tsai, A., Wei, C., Baek, H. K., Kulmacz, R. J., and Van Wart, H. E. (1997) *J. Biol. Chem.* **272,** 8885–8894
10. Tsai, A., Kulmacz, R. J., and Palmer, G. (1995) *J. Biol. Chem.* **270,** 10503–10508
11. Tsai, A., Palmer, G., Xiao, G., Swinney, D. C., and Kulmacz, R. J. (1998) *J. Biol. Chem.* **273,** 3888–3894
12. Kulmacz, R. J., Ren, Y., Tsai, A.-L., and Palmer, G. (1990) *Biochemistry* **29,** 8760–8771
13. Tsai, A., Palmer, G., and Kulmacz, R. J. (1992) *J. Biol. Chem.* **267,** 17753–17759
14. Lassmann, G., Odenwaller, R., Curtis, J. F., DeGray, J. A., Mason, R. P., Marnett, L. J., and Eling, T. E. (1991) *J. Biol. Chem.* **266,** 20045–20055
15. DeGray, J. A., Lassmann, G., Curtis, J. F., Kennedy, T. A., Marnett, L. J., Eling, T. E., and Mason, R. P. (1992) *J. Biol. Chem.* **267,** 23583–23588
16. Xiao, G., Tsai, A.-L., Palmer, G., Boyar, W. C., Marshall, P. J., and Kulmacz, R. J. (1997) *Biochemistry* **36,** 1836–1845
17. Kulmacz, R. J. Palmer, G., and Tsai, A-L. (1991) *Mol. Pharmacol.* **40,** 833–837
18. Tsai, A., Hsi, L. C., Kulmacz, R. J., Palmer, G., and Smith, W. L. (1994) *J. Biol. Chem.* **269,** 5085–5091
19. Tsai, A.-L., Berka, V., Kulmacz, R. J., Wu, G., and Palmer G. (1998) *Anal. Biochem.* **264,** 165–171
20. Kulmacz, R. J., and Lands, W. E. M. (1987) in *Prostaglandins and Related Substances: A Practical Approach* (Benedetto, C., McDonald-Gibson, R. G., Nigam, S., and Slater, T. F., eds) pp. 209–227, IRL Press, Washington, D. C.
21. Kulmacz, R. J., and Wang, L.-H. (1995) *J. Biol. Chem.* **270,** 24019–24023
22. Tsai, A.-L., Wu, G., and Kulmacz, R. J. (1997) *Biochemistry* **36,** 13085–13094
23. Stubbe, J., and van der Donk, W. A. (1998) *Chem. Rev.* **98,** 705–762
24. Hsi, L. C., Hoganson, C. W., Babcock, G. T., and Smith, W. L. (1994) *Biochem. Biophys. Res. Commun.* **202,** 1592–1598
25. Wu, G., Wei, C., Kulmacz, R. J., Osawa, Y., and Tsai, A.-L. (1999) *J. Biol. Chem.* **274,** 9231–9237
26. Lu, G, Tsai, A.-L., Van Wart, H. E., and Kulmacz, R. J. (1999) *J. Biol. Chem.* **274,** 16162–16167